Cement Well Logging Using Neutron Activation Analysis

A Major Qualifying Project Submitted to the Faculty of

WORCESTER POLYTECHNIC INSTITUTE

in partial fulfillment of the requirements for the

Degree of Bachelor of Science

By

Shane Waterman

Dr. David C. Medich, Advisor

Dr. Peter Miraglia, Co-Advisor

Abstract

The Macondo Oil Well incident in the Gulf of Mexico that began on April 20, 2010 highlighted the need for new well logging techniques to avoid future disasters. Current well logging techniques can probe well properties such as cement adhesion to the steel liner, porosity of the surrounding formation, and the bulk electrical properties of the formation. There is no state of the art technique to test for common well issues such as voids or poor centralization. This project proposes adding a neutron absorbing tagging agent to the concrete and subsequently applying the method of neutron activation analysis to detect well issues beyond what it is currently possible. This investigation showed the feasibility of this method and found an upper detection limit on emitted gamma rays. A brief discussion is also provided on future research paths to pursue in order to make this project physically realizable.

Contents

Introduction **5**

The Macondo Oil Well Incident . . . 5

Well Logging Techniques . . . 6

Resistivity Log . . . 6

Caliper Log . . . 6

Cement Bond Log . . . 6

Gamma Log . . . 6

NMR Log . . . 7

Basic Nuclear Physics . . . 7

Neutron Activation Analysis . . . 8

The Monte Carlo Code . . . 10

Proposed Method . . . 10

Methods **11**

MCNP . . . 11

Neutron Attenuation . . . 12

Determination of Ideal Tagging Agent . . . 12

Problem Geometry for Attenuation . . . 13

Problem Materials . . . 13

^{127}I Concentration . . . 14

Neutron Attenuation Calculations . . . 15

Neutron Scatter . . . 16

Neutron Dispersion . . . 16

Neutron Source in Dispersion Calculations . . . 16

Problem Geometry for Dispersion . . . 17

Neutron Dispersion Calculations . . . 17

Full Well Geometry . . . 17

Problem Geometry for Full Well . . . 18

Calculations with Dispersion and Attenuation Present . . . 18

Results **19**

Neutron Attenuation . . . 19

Neutron Dispersion . . . 20

Results from Full Geometry . . . 21

Discussion **22**

Future Work **23**

Neutron Sources 23

Neutron Moderator 23

Addition of Materials 24

Appendix A: Sample MCNP code **25**

Appendix B: MCNP Code: Neutron Attenuation by Concrete **28**

Appendix C: MCNP Code: Neutron Dispersion **31**

Appendix D: MCNP Code: Both Dispersion and Attenuation Present **34**

Appendix E: MATLAB code used to plot MCNP results **37**

Appendix F: MATLAB code used to theoretically predict activations **39**

References **41**

List of Figures

1 Wells drilled as a function of depth between the years 1940-2010 5
2 The general behavior for the activity of the activated isotope as a function of time 9
3 Depiction of the proposed well logging technique 10
4 Geometry modeled to isolate neutron attenuation effects 13
5 Geometry modeled to isolate neutron dispersion effects 17
6 Cross sectional view of concrete annulus 18
7 Attenuation Analysis for three sets of materials 19
8 Analysis of neutron flux to determine effects of scatter 20
9 Analysis of Neutron Dispersion for thermal neutron point source 20
10 Predicted results including both attenuation and dispersion 21
11 MCNP results including both attenuation and dispersion 21
12 Activations due to Iodine in the tagged concrete model 22
13 Neutron spectrum of ^{241}Americium/Beryllium 23
14 Neutron spectrum of Cf-252 24

List of Tables

1 Characteristics of ^{127}I 13
2 KENO Regular Mix Concrete Model used in this investigation 14
3 Bulk properties of the component isotopes in the model concrete 15
4 Thermal cross section comparisons for isotopes in the concrete model used 16

Introduction

The Macondo Oil Well incident in the Gulf of Mexico highlighted the need for new oil well logging techniques. Oil well logging refers to the idea of using non-invasive testing methods to gain information about properties of an oil well. There are a variety of methods currently available; for example, resistivity logs use electrical signals to measure the resistance of different materials in layers surrounding the oil well [15]. Currently, no state of the art technique exists that provides information regarding common oil well defects such as poor centralization, voids, or mixing of earth and concrete materials. This project proposes that the addition of a tagging agent to the concrete and applying the method of Neutron Activation Analysis can detect voids in the concrete. Specifically, the feasibility and an estimation of detection limits are demonstrated.

The Macondo Oil Well Incident

The Macondo Oil Well Incident began on April 20, 2010 when the steel liner of the oil well was compromised due to lack of concrete support leading to a pressurized surge of hydrocarbons rushing to the barge surface. A subsequent on-deck explosion led to the deaths of 11 barge workers and 205.8 million gallons of oil leaking into the ocean over a course of 87 days [6] [10]. The far-reaching effects of the spill are observed even today in the Gulf of Mexico's natural habitats. Though many violations of protocol and breaches of regulation were found to have occurred, it was determined that "... flaws in the planning, execution, and verification in the cement program are the precipitating cause of the incident." [1]

The depth, wall fragility, and excessive pressure surrounding the well made the Macondo Oil Well a high-risk project from the start. Developments in scanning technologies has led to a substantial increase in the drilling of these high risk wells over the past 30 years as seen in the figure below:[10]

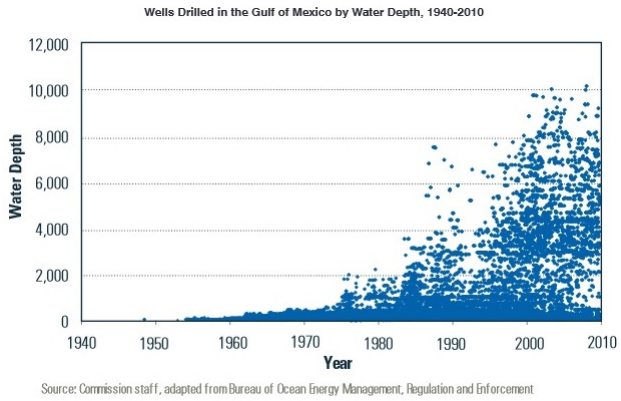

Figure 1: Wells drilled as a function of depth between the years 1940-2010

As energy demand increases in the coming years, this trend will likely continue on its current path. Thus, it is imperative that the integrity of these wells are verified prior to oil collection so further tragedies like the Macondo incident can be avoided in the future.

[1] National Commission on the BP Deepwater Horizon Oil Spill and Offshore Drilling, p.72

Well Logging Techniques

As noted earlier, several well logging techniques are currently in use to test a variety of an oil wells properties. The first well log was generated in September of 1927 by the two brothers, Conrad and Marcel Schlumberger. The brothers invented and demonstrated the applicability of the resistivity log, a technique that measures the electrical properties of the geological formations that are drilled into [14]. Since the Schlumberger brothers innovation, dozens of logging techniques have been used to test different well characterstics. The general classes of well logs is discussed below.

Resistivity Log

Resistivity Logging is used mainly in formation evaluation and works by putting a series of electrodes in contact with a geological formation of interest. These electrodes then measure the electrical resistivity of the formation, a property characteristic of a material that quantifies the materials resistance to the flow of electrical current. Most formation fluids are highly conductive and let electrical current flow freely through. Hydrocarbons are an exception, having an electrical resistance like that of an insulator. Thus, formations high in hydrocarbons will have a substantially higher resistivity than one filled with salt water [12]. Variations of the basic resistivity log are used when specialized information is desired about a certain region [3].

Caliper Log

Caliper logs are used in formation evaluation to measure the bores geometric characteristics. The tool generally has multiple adjustable arms that can sense the radius of the bore [18]. Using multiple arms allows averaging over the radii of the bore to give a mean diameter. The primary information that can be gained from Caliper Logging is a diameter profile of a well as well as pinpointing regions of damaged formation.

Cement Bond Log

Cement Bond Logs provide information about the material boundaries present in a formation. A transducer is placed down a borehole and emits ultrasonic waves into the surrounding formation. When these sonic waves hit an interface between two materials, part of the incident wave is reflected back towards the transducer while the rest of the wave propagates forward. The reflected wave is then detected at the position of the transducer. The total time of this process is then correlated to a depth at which the reflection occurred. The intensity of the reflected wave can also be correlated to the material at the interface. [18]

Gamma Log

Gamma logs are widely used in formation evaluation. Quartz rock is known to not have any natural radioactive elements in its composition. Therefore a gamma detector lowered into a borehole that passes through a shale stone region would detect little to no signal. Shale stones have a high concentration of Potassium which are natural gamma emitters. Therefore the boundaries between shale and quartz layers can be well identified by a difference

in signal intensity. Other sedimentary layers have different concentrations of radioactive isotopes and thus can also be discerned. [4]

NMR Log

Nuclear Magnetic Resonance (NMR) Logs are used to measure a formations porosity and permeability. These logs use the familiar technique of Nuclear Magnetic Resonance and the high concentration of water in formations. Hydrocarbons have an even higher concentration of hydrogen than formation water and therefore provide an increased resonance spike in the log read out. NMR Logs are especially useful in high-resistivity, sandstone regions where other logs provide limited information about the surrounding formation.[16]

Basic Nuclear Physics

The attenuation of an incident flux of neutrons in one dimension is quantified by the flux survival equation:

$$\Phi(L) = \Phi_0 e^{-\Sigma_a L} \tag{1}$$

Where $\Phi(L)$ and Φ_0 are the flux a distance L into the material and incident flux, respectively. Σ_a is the macroscopic absorption cross section a macroscopic material property which quantifies the amount of neutrons attenuated by absorption processes per unit length traveled. It can be defined as the following:

$$\Sigma_a = \sigma_a N \tag{2}$$

σ_a is the microscopic thermal absorption cross section measured in units of barns (10^{-24}-cm^2). The microscopic cross section describes the probability that an incident neutron will undergo an absorption process with the target nuclei. Despite having units of barns, it is not a physical area. Instead, it is an effective cross sectional area where a larger cross section is indicative of a higher probability of interaction. The cross section depends on the nature of the incident radiation (α, β, γ), the interaction process of interest, and the energy of the incident particle. In general, the neutron absorption cross section increases as thermal energies are approached. A typical neutron source will have a spectrum of energies, thermal neutrons only comprising a small percentage of the total spectrum. This phase of the analysis will assume fully thermalized neutrons (an idealization which will never be realized, but for analytical purposes with be assumed). Every interaction process has an accompanying cross section. Combinations of cross sections scale linearly and therefore a total cross section can be defined:

$$\sigma = \sum_{i=1}^{N} \sigma_i \tag{3}$$

For the analysis considered in this investigation, only the absorption cross section will be considered. As will be shown, neutron scatter complicates the situation dramatically because the incident neutrons will be scattered off their initial trajectories. When this occurs, the neutrons path length is increased and a higher probability of absorption is observed than predicted as it travels through more material.

The second parameter in equation 2 is the atomic density of the material, N. This quantifies the number of target atoms in a given volume of interest and will be used in units of atoms/barn/cm to stay consistent with

MCNP. Mathematically it is defined as:

$$N = \frac{\gamma \rho_m N_A}{m} \tag{4}$$

In equation 4, γ is the weight fraction of the element of interest, ρ_m is the composite material density, N_A is Avogadro's constant equal to 6.022*10^{23} atoms/mole), and m is the molar mass of the element. For a composite material, the individual atomic densities are additive. If an "impurity" to the material such that it constitutes a weigh fraction, p, in the material then the weight fractions of the other materials will scale by a factor (1-p).

Using equations 4, equation 2 can be rewritten as:

$$\Sigma_a = \frac{\gamma \rho_m N_A}{m} \sigma_a \tag{5}$$

This form of equation 2 is more convenient to work with since all the parameters are known. It should also be noted that, in this investigation, Σ_a and σ_a are the macroscopic and microscopic thermal neutron absorption cross sections, respectively. [17]

Neutron Activation Analysis

Assume that a sample initially holds N_T stable ${}^{A}_{Z}X$ target atoms with a microscopic absorption cross-section, σ_a. These target atoms are exposed to a uniform beam of mono-energetic neutrons with a fluence rate equal to $\dot{\Phi}$. The target isotopes will absorb a certain portion of the incident neutrons and form isotopes of the target nuclides, ${}^{A+1}_{Z}X$. The production rate of the activated isotopes is then simply given by:

$$\dot{N} = \dot{\Phi} \sigma N_T \tag{6}$$

where N is the number of activated isotopes (${}^{A+1}_{Z}X$) in the sample after a time, t. The differential equation governing the number of activated isotopes in the sample at a time, t, is given by:

$$\frac{dN}{dt} = \dot{\Phi} \sigma N_T - \lambda N \tag{7}$$

In this equation, λ is the decay constant of the activated isotopes. Thus, the second term on the right-hand side is simply the number of activated isotopes that decay into their daughter nuclides. For a poly-energetic beam of incident neutrons, the solution can be approximated by binning the incident beam into a series of mono-energetic groups. Each group will have a corresponding fluence rate and cross-section, yielding a set of ordinary differential equations identical to equation 7. This can be done to higher and higher accuracy using computational methods.

For the mono-energetic case, it will be assumed that $\dot{\Phi}$ remains unchanged over the thickness of the material of interest and that the target atom population is large enough that it is not appreciably reduced (i.e. $\dot{\Phi}$ and N_T have no functional dependence on time and can thus be taken as constants). These assumptions set the first term on the right-hand side to be a constant.

The differential equation is now solved by using a trial solution of the form:

$$N = a + be^{-\lambda t} \tag{8}$$

Both a and b are constants determined by conditions set on the problem. If it is assumed that there are no daughter isotopes in the sample prior to irradiation (imposing the initial condition, N=0 at t=0), the constants can be solved

for. The number of activated isotopes in the sample as a function of time is found to be:

$$N(t) = \frac{\dot{\Phi}\sigma_a N_T}{\lambda}(1 - e^{-\lambda t}) \tag{9}$$

Recognizing that the activity of a sample is the numer of atoms in that sample multiplied by its respective decay constant, the activity of the daughter isotope is:

$$A(t) = \dot{\Phi}\sigma_a N_T(1 - e^{-\lambda t}) \tag{10}$$

Plotting the general behavior of this activity curve, a saturation effect is seen to occur:

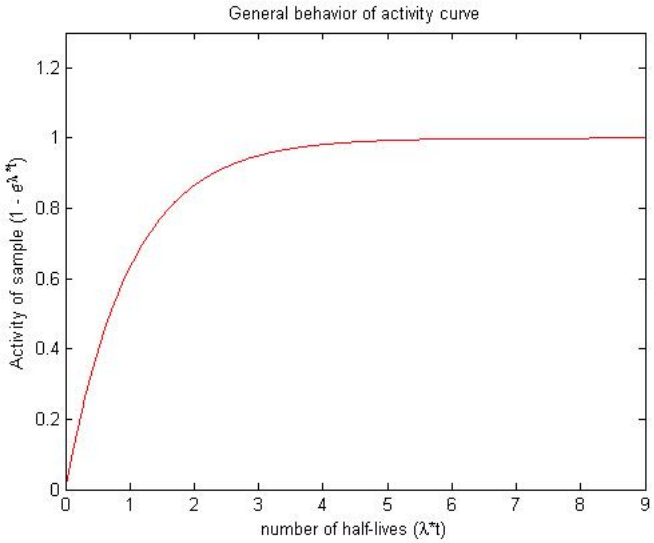

Figure 2: The general behavior for the activity of the activated isotope as a function of time

The saturation activity of the irradiated sample can be solved for by considered what happens as t grows large. As t increases, the exponential term in the parentheses approaches zero leaving only the pre-factor. Explicitly:

$$A_{sat} = \dot{\Phi}\sigma_a N_T \tag{11}$$

This equation can be expressed in terms of macroscopic parameters as follows:

$$A_{sat} = \dot{\Phi}\Sigma_a V \tag{12}$$

N being the volume that the target atoms occupy. The energies and relative intensities of radioactive decay products are well known for the isotopes of each element. It is also known that gamma-rays of a radioactive species are characteristic of their parent nuclides. Thus, the gamma-rays of the irradiated sample can be measured and compared to perform gamma spectroscopy on the sample. If a certain isotope is in the sample, higher count rates will be observed at the energies of its characteristic gamma rays. The relative intensity of these elevated count rates would be proportional to the concentration of that isotope in the sample. [11] [17]

The Monte Carlo Code

The Monte Carlo N-Particle (MCNP) code was developed by Los Alamos National Laboratory to model the stochastic process of particle transport. The user creates an input file with the specified problem geometry, materials of interest and their accompanying cross-section tables, position and characteristics of the radiation source, and the information they wish to obtain from the simulation. The program reads the input file and generates a source particle at the specified location. The interactions of the particles in the problem materials are modeled using normalized probability density functions. A random number generator is used to generate a number between 0 and 1 which is then correlated with an interaction. If the particles track is not terminated (e.g. not absorbed), the random number generation process further dictates the particles behavior until it is either absorbed or leaves the defined region. When a particle interacts in a region of interest, its behavior is tracked and recorded. Once all particle histories have been carried out, the overall result is normalized to a single source particle.

The user specifies the information they wish to obtain by placing a tally on a surface or volume of interest. MCNP has a series of built-in tallies that can measure quantities such as particle flux over a surface or averaged through a volume, energy deposition in a material, or flux at a detector. These results are then printed in an output file along with the results associated error, calculated using standard counting statistics. If the problem geometry is not well specified, a small error is not necessarily indicative of the quality of the result. Therefore, care must be taken to accurately and efficiently setup the problem. If used properly, MCNP is a powerful tool that can be used to solve problems for which an analytic solution is either incredibly difficult or simply does not exist. [7]

Proposed Method

This investigation proposes that volumetric defects can be discovered in the cement annulus surrounding an oil well using Neutron Activation Analysis. This general concept is summarized in the figure below:

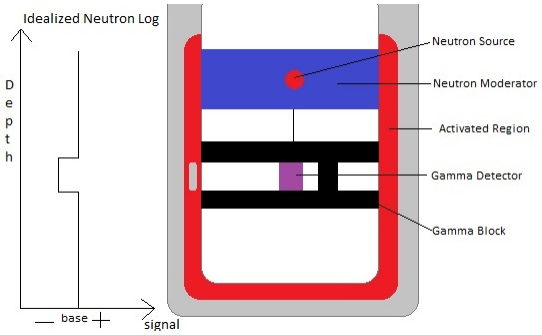

Figure 3: Depiction of the proposed well logging technique

Initially, a poly-energetic neutron source surrounded by a neutron moderating material is lowered into the well. As the neutrons travel through the moderator, their energies are lowered to thermal energies ($E_{thermal}$ = .0253 eV) by means of energy transfer mechanisms such as scatter. These neutrons then traverse into the annulus filled with concrete doped with a tagging agent. The incident neutrons absorbed which activates the concrete. The excited isotopes decay and emit a gamma particle in the process. Attached below the neutron source is a gamma detector

isolated by a series of gamma blocking materials. These materials are in place to isolate the detector such that only a specific region of the annulus is focused upon at a given time.

In figure 3, the idealized neutron log on the left provides a graphical representation of the information collected by the gamma detector. The base signal is the signal that would be obtained for the ideal density and volume of concrete desired. The detector would register a drop in signal if a region containing a void were passed by the detector. The addition of a gamma blocking material between the top and bottom blocking layers could then further isolate a void by zoning in on a specific slice of the cement annulus. The entire detector setup could be made to rotate so that collected information is maximized.

Methods

This investigation used both analytical and computational techniques to model a cement annulus around an oil well doped with a neutron absorbent tagging agent. As dicussed in the previous section, the radiation transport code used was the MCNP6 Monte Carlo environment developed by Los Alamos National Laboratory. Analytical, numerical, and graphical work was done using MATLAB R2013B developed by MathWorks [8]. The vast majority of this project was devoted to developing a working, realistic model of the problem geometry. The remainder was devoted to using available resources to carry out a feasible analysis and quantifying detection limitations of the proposed method. Finally, future goals were identified and possible research paths were touched upon.

The first aspect of this project was to consider how neutrons were attenuated as they traveled through the cement. In order to do this, a model for concrete had to be chosen, a suitable tagging agent had to be decided upon, and a problem geometry had to be constructed that isolated the effects of neutron attenuation. A series of MCNP simulations were then carried out and compared to analytically obtained attenuation values. These simulations highlighted the unexpected effect neutron scatter would have in this problem. Thus, the same process had to be carried out in order to isolate and quantify the impact neutron scatter would have on the problem. The second major portion of this project was concerned with the effects that neutron dispersion would have. Again, the effect was isolated from that of attenuation and studied. Finally, these situations were combined to see how the incident neutrons interacted in the cylindrical geometry with attenuation, dispersion, and scatter each playing their respective role.

MCNP

MCNP6 was used to perform particle transport simulations for the computational aspect of this investigation. A series of different geometries were used to fit specific purposes as will be discussed shortly. Thermal neutrons were generated using the standard SDEF card for both the point source and directed plane source. The cross section tables used were the endf70c neutron cross section tables supplied with MCNP6. For surface flux tallies, the F2 surface flux tally was used. For the activation analyses, the F4 tally was used which measures the cell averaged volume flux. This was subsequently modified by the FM multiplier card to give ^{127}I activations/barn/cm. These were used in conjunction with the FMesh tally which is used to setup a series of adjacent tallies. As will be discussed later, concrete was modeled using the KENO Regular Mix Model taken from Appendix D of the MCNP Criticality

Primer. Simulations were run for $1x10^7$ particle histories to obtain a tally error less than 5 %. A heavily-commented sample MCNP code that describes the different MCNP syntax used in this investigation can be seen in Appendix A.

Neutron Attenuation

Determination of Ideal Tagging Agent

Previous investigations into the question of what tagging agent to use were considered by Dr. Peter Miraglia and can be found in reference [9]. The tagging agent was chosen based on the following criteria:

1. The activated isotope of the tagging agent will have a gamma ray in it's decay
2. The emitted gamma ray will have sufficient energy such that it is not appreciably attenuated through the cement annulus
3. The nuclide will have a high enough thermal absorption cross section such that there is a detectable increase in gamma rays
4. The activated radioisotope will have a sufficiently long half life such that the activated population did not decay substantially prior to detection

Condition (1) is desired because, as was noted in the section on Neutron Activation Analysis, the energy of an emitted gamma is characteristic of the parent nuclide. This allows for the detector to be calibrated to that energy range and the resultant signal due to the tagging agent can be isolated. Condition (2) ensures that every gamma emitted in the direction of the detector has the ability to be detected. Condition (3) is needed because the proposed method relies on there being an increased signal. An increasae in emitted gammas is primely dependent on the parent nuclide's thermal neutron absorption cross section. Condition (4) is required because, if all the activated isotopes decayed prior to detection, there would be no difference between normal and doped concrete.

Dr. Miraglia's investigation found a patent registered by Frederick Rambow of the Shell Oil Company in 1989 that used Iodine as a tagging agent to determine the thickness of the cement annulus of an oil well [13]. ^{127}I has a thermal neutron cross section of 6.15 barns and, upon neutron absorption, transforms to ^{128}I. ^{128}I has a half-life of 3.5 hours and decays via beta emission with an accompanying gamma ray with an energy of .442 MeV. In terms of the isotopes of Iodine, ^{127}I has a natural abundance of 100% and thus no generator would need to be used. Therefore, ^{127}I was determined to be the ideal candidate. The above data is summarized in the table below:

Tagging Agent	^{127}I
σ_a [thermal] (barns)	6.15
Natural Abundance (%)	100
Activated Isotope	^{128}I
$t_{1/2}$ (hours)	3.5
Decay mode	β, γ
E_γ (MeV)	.442

Table 1: Characteristics of ^{127}I

Problem Geometry for Attenuation

To isolate neutron attenuation effects, a non-dispersive neutron source had to be modeled. The simplest way to block out dispersion effects is to model a directed neutron source. This makes it so that the neutrons direction of travel is predefined and is no longer a probabilistic process. A cement slab was used as the target material and a plane source was generated parallel to the front face of the slab. The cross-sectional area of the source was equal to the front face of the slab. This was all done to ensure that every simulated neutron was incident on the concrete slab. This geometry is shown in the figure below:

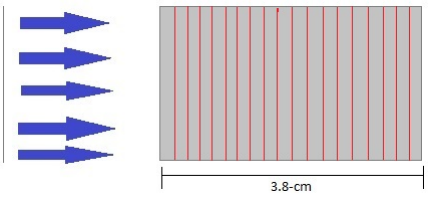

Figure 4: Geometry modeled to isolate neutron attenuation effects

The thickness of the slab was chosen to equal that of the Macondo well's thickness at the point of compromise. The red lines in figure 4 are a representation of how a mesh tally is used.

Problem Materials

Oil wells have two main components to them that allow hydrocarbons to flow in the bored out region. On the inside of the well is a steel tube that runs the length of the well. Outside the steel but inside the bore is the concrete annulus that is poured on sight as structural support for the inner steel liner. The concrete acts to offset the pressure on the well from the surrounding geological formation. The structural stability of the well is heavily reliant on the integrity of the concrete. Issues such as voids or poor centralization can have compromising effects on the well and lead to a blowout. The thinness of the steel liner and lack of neutron and gamma absorbing properties allowed for consideration of solely concrete. The model used for concrete was taken from Appendix D of the MCNP Criticality Primer provided with the MCNP6 source code [7]. Out of the three concrete models provided, KENO Regular Mix Concrete was the simplest while still having the basic components expected (SiO_2, Al_2O_3). The KENO Regular

Mix has the following composition:

Element	Composition Proportion	Molar Mass (g/mole)
H-1	.01	1.0797
O-16	.532	15.9994
Na-23	.029	22.9898
Al-27	.034	26.9815
Si-28	.337	28.086
Ca-40	.044	40.08
Fe-56	.014	55.847

Table 2: KENO Regular Mix Concrete Model used in this investigation

^{127}I Concentration

The tagging agent concentration was determined such that the following criteria were met:

1. The incident neutron beam is not significantly attenuated
2. The tagging agent concentration will not alter the chemical properties of the concrete
3. The resultant signal is maximized

The first restriction is needed because, if the neutron beam is significantly attenuated, there will be a disproportionate weighting of activations through the concrete and the resulting log will preferentially provide information about the inner radii of the annulus. The goal is to obtain the maximum information about the entire volume of concrete and therefore a uniform distribution of activations is desired. To quantify restriction (1), a target total attenuation through the concrete thickness of 5% was decided upon. Restriction (2) is necessary because the tagged concrete needs to be able to provide the same support as the untagged concrete. Restriction (3) is needed to make the proposed method as efficient as possible. Obviously, higher concentrations of ^{127}I would provide higher signals. However, restrictions (1) and (2) would then not be met and the method fails. Therefore, there exists a theoretical limit where all three conditions are optimized.

The optimal tagging agent concentration was found by first looking at the standard flux survival equation:

$$\Phi(L) = \Phi_0 e^{-\Sigma_a L} \tag{13}$$

This equation was rearranged and Σ_a was expressed in terms of micrscopic parameters via equation 5 to give:

$$-ln\left(\frac{\Phi(L)}{\Phi_0}\right) = (L\rho_m N_A)\left(\frac{p\sigma_I}{m_I} + \sum_{i=1}^{N}\frac{(1-p)\gamma_i\sigma_i}{m_i}\right) \tag{14}$$

The argument of the natural logarithm on the left hand side of the above is equation is the target survival percentage of the incident neutron flux. From restriction (1) above, this value was set to 95% (given a 5% attenuation). In the first set of parentheses on the right hand side, L is the concrete thickness, ρ_m is the composite concrete mass

density, and N_A is Avogadro's constant. In the second set of parentheses, the first term is the contribution to the attenuation from Iodine. The second term is the contribution to the attenuation from the added ^{127}I with weight fraction p. The sum on the right side is the scaled contribution to the attenuation from the concrete. Since p is a constant, it can be taken out of the sum and solved for to get an expression for the optimal weight fraction of the added ^{127}I as follows:

$$p = \frac{\frac{-ln\left(\frac{\Phi(L)}{\Phi_0}\right)}{L\rho_m N_A} - \sum_{i=1}^{N} \frac{\sigma_i \gamma_i}{m_i}}{\frac{\sigma_I}{m_I} - \sum_{i=1}^{N} \frac{\sigma_i \gamma_i}{m_i}} \tag{15}$$

Using this equation, it was found that the optimal tagging agent concentration to satisfy the three restrictions listed above was 5.35%. To be conservative, this value as dropped to 5% to preemptively account for some inherent scatter. With p equal to 5%, the atomic densities and macroscopic thermal absorption cross sections for the composite concrete could be re-evaluated as in the table below:

Element	N (atoms/barn/cm)	Σ_a (1/cm)
H-1	.013054	.004334
O-16	.043752	8.31292 * 10^{-6}
Na-23	.001659	.000882
Al-27	.001659	.000383
Si-28	.015789	.002789
Ca-40	.001445	.000589
Fe-56	.000329	.000928
I-127	.000546	.003383
All materials	.078234	.009845

Table 3: Bulk properties of the component isotopes in the model concrete

The values in table 3 for both the atomic density and macroscopic thermal neutron absorption cross section were used in MCNP simulations as well as analytical calculations.

Neutron Attenuation Calculations

A series of MCNP simulations were conducted with the geometry seen in figure 4. Three different situations were examined. The first situation was when the slab was filled with only ^{127}I at the atomic density listed in table 3. The second and third situations are untagged and tagged concrete with the values found in table 3.

Analytical activation calculations were found using equation 12 with the flux term solely having an attenuation contribution (equation 1):

$$A_a = e^{-\Sigma_a x}\Sigma_a V \tag{16}$$

The Φ_0 from equation 1 was set to one to be in agreement with MCNP's results. The MCNP code used for these simulations can be found in Appendix B.

Neutron Scatter

Investigation of the neutron activation curves due to attenuation revealed that there was another process going on that skewed the results of the attenuation curves. It was believed that the saturation behavior was a consequence of neutron scatter within the materials. Since neutron scatter is not easily accounted for analytically, the thermal neutron absorption and scatter cross sections were compared for each of the isotopes in the concrete. This data can be seen in the table below [5]:

Element	$\sigma_{n,\gamma}$ (barns)	σ_s (barns)
H-1	.332	80
O-16	190 * 10^{-6}	3.780
Na-23	.5314	.558
Al-27	.2311	1.414
Si-28	.1767	2.149
Ca-40	.4075	3.022
Fe-56	2.813	12.46
I-127	6.2	3.540

Table 4: Thermal cross section comparisons for isotopes in the concrete model used

As expected, the only isotope for which the scatter cross section did not outweigh the absorption cross section was ^{127}I. Thus, scatter begins to plays an increasing role as more materials are added to the simulation geometry.

MCNP was used with only the F4 cell averaged flux tally to quantify the extra attenuation that was introduced because of neutron scatter. The same code seen in Appendix B without the FM tally multiplier added was used to do this.

Neutron Dispersion

The second major aspect of this project was determining the effect that neutron dispersion had on the activations in the concrete. The rectangular volume was filled with only ^{127}I to minimize the effects of attenuation and scatter. The two simulation parameters that were changed were the problem geometry and the neutron source characteristics.

Neutron Source in Dispersion Calculations

The simulations to quantify the effect of neutron dispersion used a thermal neutron point source at the origin. While the idea of a point source is an idealization, it holds when the radius of the source is small in comparison to lengths of interest. In the present case, the inner radius of the oil well is 8.9-cm while the source would be on the order of millimeters so the point source approximation is valid to high precision.

Problem Geometry for Dispersion

The geometry used for dispersion calculations had to be such that neutron attenuation was minimized. Thus, a thin rectangular volume was generated that extended along the y-axis. The source was a distance of 8.9-cm in the x-direction from the center of the rectangle. A mesh tally was used that divided the rectangle into a series of equal volume cells in the y-direction. A representation of the geometry used is seen in the figure below:

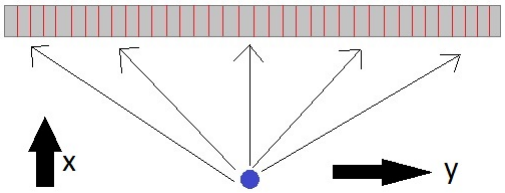

Figure 5: Geometry modeled to isolate neutron dispersion effects

It should be noted that the size of the neutron source in figure 5 is exaggerated to highlight the position and emission geometry of the neutrons. The MCNP code used for the dispersion simulations can be seen in Appendix C.

Neutron Dispersion Calculations

Equation 12 was used to analytically predict the number of expected activations using the geometry in figure 5. The point source approximation suggests a spherically symmetric emission spectrum of neutrons and thus the flux term would be written:

$$\Phi(R) = \frac{\Phi_0}{4\pi R^2} \tag{17}$$

Where $\Phi(R)$ is the flux at a radial distance R away from the source and Φ_0 is the initial flux. To compare analytical and MCNP results, Φ_0 was set equal to one for a single source particle. The inverse of the sphere area is due to there being an equal probability of an incident neutron passing through any point on a sphere of radius R centered at the origin. Thus, the activation equation can be written as:

$$A_d = \frac{1}{4\pi R^2}\Sigma_a V \tag{18}$$

This equation was used to compare the predicted results to the results obtained from MCNP.

Full Well Geometry

With the effects of neutron attenuation and dispersion well understood, the final step was to combine the effects in the full well geometry to see the detection limit of the proposed method. The tagging agent, problem materials, and percent compositions were kept the same as the previous two situations. The source was kept as a thermal neutron point source. What did change was the problem geometry as will be discussed.

Problem Geometry for Full Well

The full geometry of the oil well is a concrete annulus separating an inner air region from an exterior earth region. The spherically symmetric emission spectrum of the neutron source allowed for the collapse of the concrete annulus down to that of a thin concrete slab. This is due to the fact that there is no dependence on the azimuthal angle from the source; only the radius and polar angle play a role in determining the flux at a point. This can be visualized using the figure below:

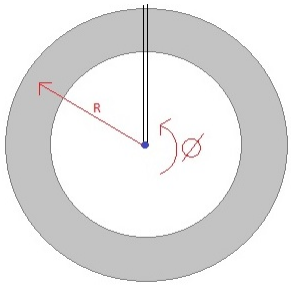

Figure 6: Cross sectional view of concrete annulus

The region in figure 6 blocked off by the two vertical black lines is an example of a rectangular region that can be summed over to give the full annulus.

Thus, the entire concrete annulus can be constructed by summing together a series of thin rectangular cells. Obviously some error will be introduced since there will be added corner effects as the rectangles form a circle. As with Riemannian sums however, smaller rectangles will lead to smaller errors. Models with finer geometrical constructions would need to be generated in order to closer replicate the MCNP model. As neutron scatter plays an ever increasing role however, the MCNP Results will diverge from the analytical model derived in this investigation. For present purposes then, the rectangular subdivisions will suffice to provide a working analytical model to compare against MCNP.

Calculations with Dispersion and Attenuation Present

Neutron dispersion is a geometric effect that originates in the geometry of the neutron source. Neutron attenuation, on the other hand, is an effect due to the materials present in the problem. The relative independence of these two effects allows for the combination of them as a product to give the full flux term:

$$A = \Phi_a \Phi_d \Sigma_a V = \frac{1}{4\pi R^2} e^{-\Sigma_a x} \Sigma_a V \tag{19}$$

To avoid ambiguity, R is the radial distance of the point of interest *from the source* while x is the distance the neutron has traveled in the material with macroscopic thermal absorption cross section Σ_a.

The MCNP model generated used a thermal neutron point source and had a concrete slab with a mesh tally in two dimensions. Thus, depth in the slab and radial distance from the source were both accounted for. The MCNP model used can be found in Appendix D. MATLAB was used to do iterated calculations and to generate surface

plots of the activations in the slab. The MATLAB code used to do these tasks can be found in Appendix E.

The results of the mesh tally in this section for the Iodine-tagged Concrete and the untagged concrete were then subtracted from each other. This was done to see how many activations were due to the Iodine tag for each of the cell volumes in the mesh tally. These results were then scaled from a single source particle to a 1 Curie(Ci) source (1 Ci = $3.7*10^{10}$ decays/second) in order to provide a more realistic perspective. This also provided information on how many detectable gamma rays would be emitted once the ^{128}I began to decay.

Results

Neutron Attenuation

The data obtained by simulating the geometry in figure 4 is seen in the figure below:

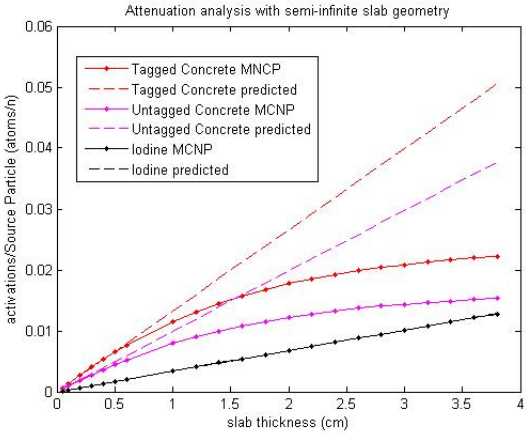

Figure 7: Attenuation Analysis for three sets of materials

In this figure, the MCNP results are plotted along with the analytically predicted results. The simplest case, where the slab is filled only with ^{127}I shows that the predicted and simulation results are effectively indiscernible. As materials are added, a divergence between predicted and simulation result is observed and the MCNP results show the neutron activations saturating through the slab thickness. The argument was made that this was due to neutron scatter and a discussion on that topic is seen in the section under methods entitled "Neutron Scatter".

Neutron Scatter

The data obtained by MCNP simulations for the flux tally and the predicted results using equation 19 were compared. This data is shown in the figure below:

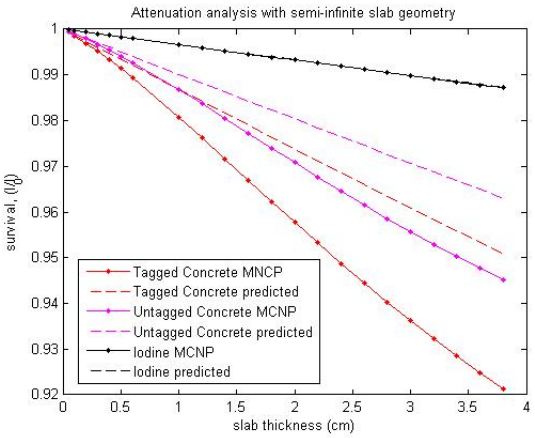

Figure 8: Analysis of neutron flux to determine effects of scatter

As in the section of activations due to neutron attenuation, the results of the Iodine filled volume with MCNP and equation 1 are indiscernible. As materials are added, it is seen that the neutron flux falls off faster than initially predicted. As neutrons scatter, their path length is increased and their probability of absorption is therefore increased. The neutrons can also be scattered off-axis and leave the volume of interest entirely, therefore never being absorbed. Thus, a smaller flux than anticipated reaches deep into the slab and the equation 19 fails beyond roughly .5-cm in the slab. This shows the necessity of using MCNP to get accurate results.

Neutron Dispersion

The effects of neutron dispersion were calculated using equation 18 and compared to the MCNP results:

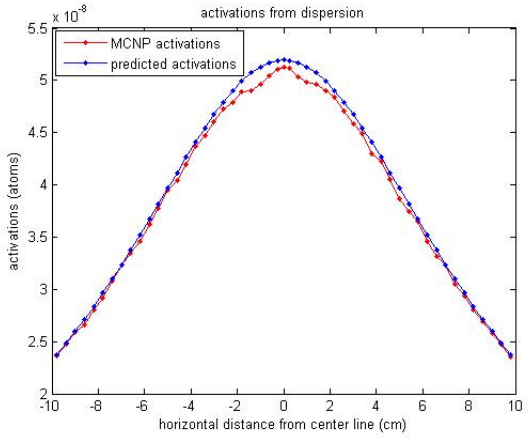

Figure 9: Analysis of Neutron Dispersion for thermal neutron point source

The above graph shows great agreement between equation 18 and MCNP's results. There is slight disagreement between the two curves in the immediate area of the peaks. There has not been a conclusive decision on the cause of this as of yet. Part of this may have come from MCNP's inherent error. However, the remainder of this error is

still unknown. The majority of the two curves are still in agreement with each other leading to the conclusion that equation 18 is valid for this investigation.

Results from Full Geometry

The activation results were calculated using the MATLAB code in Appendix F which used an iterated form of equation 19. These results for tagged and untagged Concrete are shown below: As is seen, there is a significant

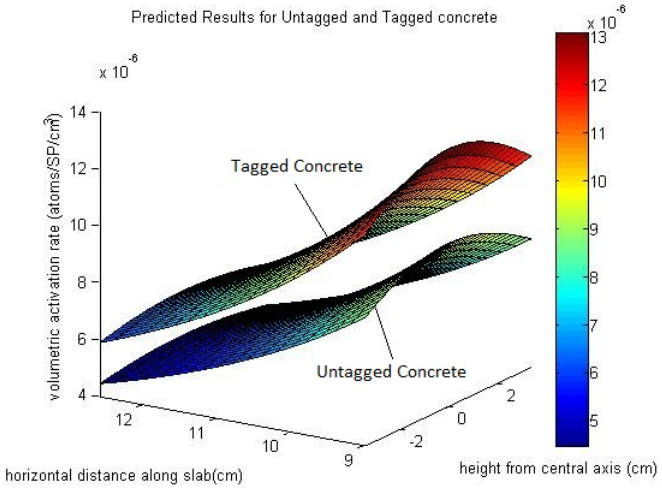

Figure 10: Predicted results including both attenuation and dispersion

difference in activations between the tagged and untagged concrete. The MCNP results are similarly plotted: Examination of figure 11 shows a substantial difference in activations between the two surfaces at the peaks and

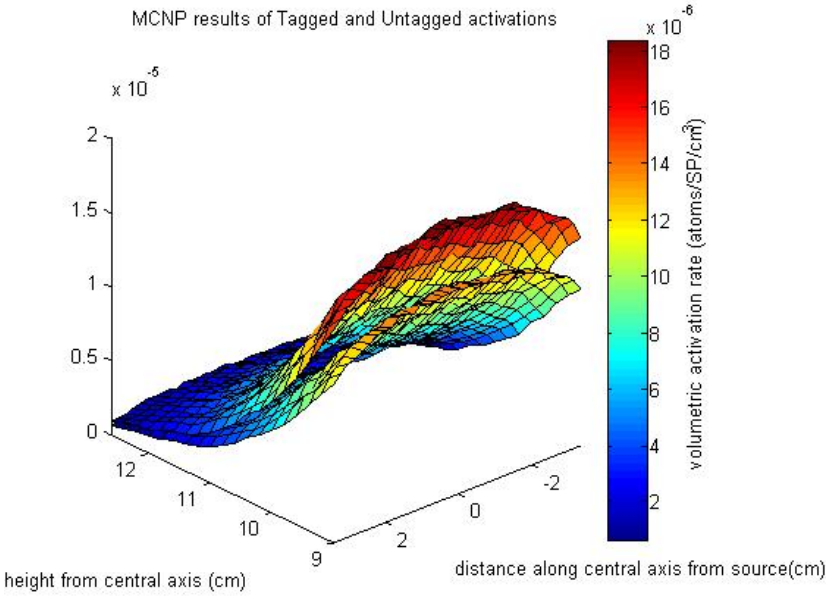

Figure 11: MCNP results including both attenuation and dispersion

along the face of the slab. As further depths into the slab are considered, the two curves begin to converge on each other as neutron scatter becomes more prominent. At the far end of the slab, the two surfaces are significantly closer than they originally were. The hope is that, when the earth region is added to model which has a high hydrogen concentration, neutrons will be back-scattered into the annulus and increase the number of Iodine activations. Comparing figures 10 and 11 shows an increase in magnitude of activations at the peak for the MCNP curves. This is an effect of the neutron scatter because incident neutrons are back-scattered towards the front of the slab from the materials that occupy the slab volume.

The difference in the activations between the two MCNP curves was calculated and is shown in the figure below: Figure 12 is scaled to a 1-Ci source to give a more realistic representation. It is seen that for at the peak for 1-Ci,

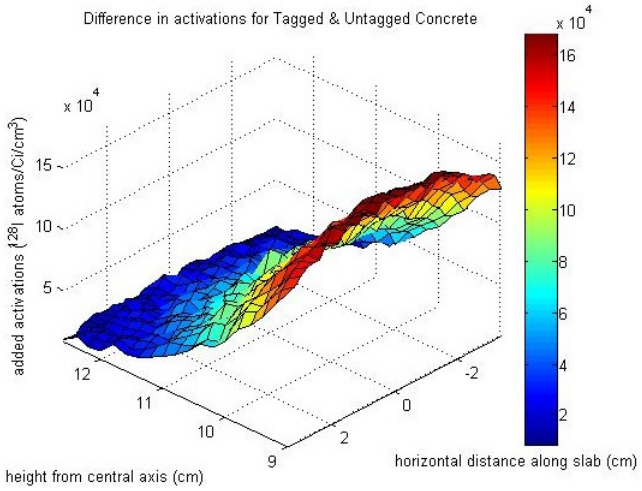

Figure 12: Activations due to Iodine in the tagged concrete model

there is an increase of roughly 18,000 detectable gamma particles. Even at the far end of the slab, there is still an increase of 2,000 detectable gammas.

Discussion

Figures 11, 10, and 12 show the significant (in that they are detectable) increase in detectable gamma particles that result from using a small concentration of Iodine-127 as a tagging agent in concrete. Figure 12 shows the feasibility of the method but also indicates some limitations that may be encountered. For example, this method will be far more sensitive for voids near the front of the annulus where the number of Iodine activations is substantially higher. Voids at the far depth of the annulus will be harder to detect since there are close to 1/9th the amount of activations compared to the front of the annulus. With the addition of earth materials, the number of Iodine activations at the far end of the annulus may increase due to back-scattered neutrons. This could help with the detectability of voids.

This method will be highly sensitive for the detection of poor centralization. The number of detected gammas can be found using MCNP and placing a tally at the center of the annulus and measuring emitted gammas. A

smaller tally result will be indicative of either a void or poor centralization, neither of which are desired. As the detector scans the region of the annulus isolated by the gamma blocks, a gradient in detected gamma intensity will be representative of poor centralization. This is because regions of high intensity will have extra concrete that should have formed around other parts of the annulus. The regions of lower intensity will mean there is less concrete in that area supporting the oil well.

Future Work

More work will need to be conducted to make neutron activation analysis a feasible method for cement well logging. Three research paths were identified as the next facet to explored. First, the thermal neutron point source idealization will have to be moved away from and a polyenergetic neutron source of finite size will need to be used. Second, a neutron moderating material will need to be decided upon. Third, more materials will need to be added to the MCNP models such as earth, shalestone, or mud. Each of these topics are discussed separately.

Neutron Sources

Two of the most common neutron sources in production are Californium-252 and ^{241}Americium/Beryllium. The neutron spctra for these two sources are shown below [1] [2]:

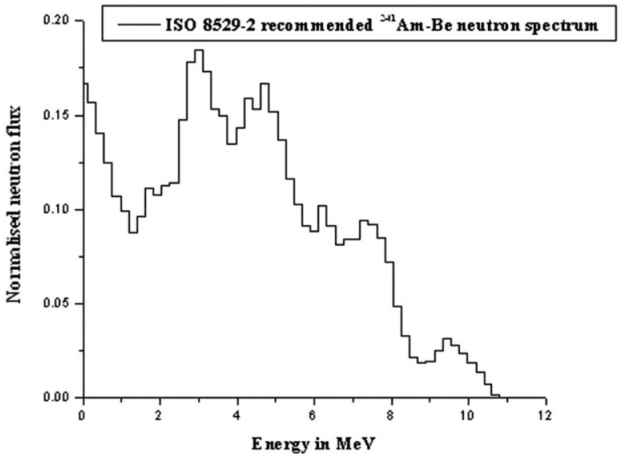

Figure 13: Neutron spectrum of ^{241}Americium/Beryllium

AmBe has a half-life of 432 years and has a wider neutron spectrum. Cf-252 has a half-life of 2.65 years and has a slightly more narrow spectrum. AmBe is also more expensive to produce. Thus, each source has their advantages and disadvantages.

Neutron Moderator

As was seen in the section on neutron scatter, neutrons scatter very readily off of Hydrogen. Thus, the ideal moderator would have a very high concentration of hydrogen atoms. For this reason, three materials being considered

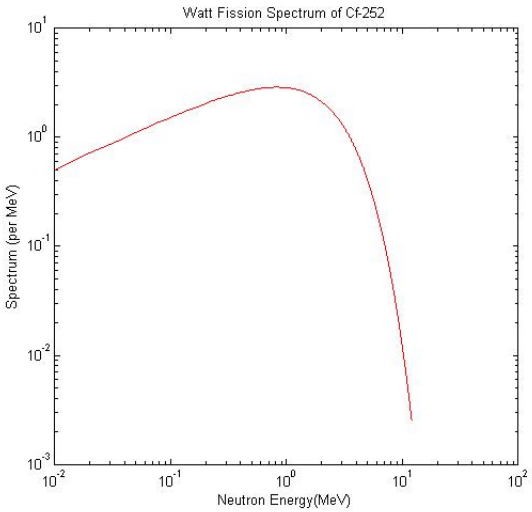

Figure 14: Neutron spectrum of Cf-252

as neutron moderators are the following:

1. High-Density Polyethylene (HDPE)
2. Heavy Water (D2O)
3. Graphite

All three materials are fairly cheap to produce in the amount needed. HDPE and Graphite both have the advantage of easily being machined to a desired shape. D2O may be slightly problematic in that shifting of fluid could cause uneven, unpredictable moderation.

Addition of Materials

An important step will be to further make the MCNP model more realistic. This will be done mainly by adding more materials to the problem geometry. This investigation only considered the concrete annulus of the well. Other materials that need to be examined are the earth regions outside of the bore region, gamma blocking materials, etc. Geological formations tend to have many different layers, each having their own signature isotopic composition. Neutrons will interact differently in each of these regions so it is imperative to understand their behavior in each region and what effect this will have on the Iodine activations.

Appendix A: Sample MCNP code

```
Slab mesh tally
c -------1---------2---------3---------4---------5---------6---------7---------8
c Analysis of neutron activation [(n,gamma) reaction] in a rectangular
c volume to test for the attenuation properties of the concrete used in this
c simulation. The neutron source was that of a directed plane source of thermal
c neutrons.
c -------1---------2---------3---------4---------5---------6---------7---------8
c Cell Cards
c The cell definition section consists mainly of the slab of concrete for this
c problem. The mass density of concrete is specified by the (-2.92) as the third
c string in the section below. The negative sign indicates a mass density is
c desired
c -------1---------2---------3---------4---------5---------6---------7---------8
10  1      -2.92      (-1)      imp:n=1    $(slab)
11  0                 (1 -100)  imp:n=1    $(external to slab)
20  0                 (100)     imp:n=0    $(end of world region)
c -------1---------2---------3---------4---------5---------6---------7---------8

c Surface Cards
c -------1---------2---------3---------4---------5---------6---------7---------8
c The geometry of interest is a 3.8-cm slab in a vacuum. The purpose is that
c attenuation will be isolated as the only effect of interest in the problem.
c -------1---------2---------3---------4---------5---------6---------7---------8
1  RPP  8.9 12.7  -1 1    -3.5 3.5
100 SO 30
c -------1---------2---------3---------4---------5---------6---------7---------8

c Data Cards
mode n
c -------1---------2---------3---------4---------5---------6---------7---------8
c Source Specification section
c The source is a directed thermal neutron plane source aimed at the front face
c of the concrete slab such that every emitted neutron is incident on the slab
c material.
SDEF  POS = 0 0 0 X=d1 Y=0 Z=d2 PAR=1 VEC=0 1 0 DIR=1 ERG=2.53e-8
SI1 -1 1
```

```
SP1 0    1
SI2 -1 1
SP2 0    1
SDEF POS = 0 0 0 ERG=2.53e-8
c ------------------------------------------------------------------------------
c The tally that will be used is a rectangular F4 mesh tally modified by
c using an FM-multiplier card. The F4 tally measures the cell-averaged neutron
c flux in the cell of interest. The FM4 modifies this tally by multiplying the
c F4 tally by the microscopic absorption cross section
c
c The syntax of the rectangular mesh tally is as follows:
c FMESHn:<pl>   where n is the cell number and <pl> is the particle designator
c ORIGIN denotes the bottom left corner of the rectangle of that the tally will
c be defined in.
c IMESH is the placement along the x-axis of the coarse mesh points
c IINTS is the number of fine mesh points (bins) between the coarse mesh points.
c In the tally below, there are 19 bins being placed between 8.9-cm and 12.7-cm
c in the X direction.
c JMESH is the same as IMESH except in the y-axis.
c KMESH is the coarse mesh point in the z-axis
c
c The first entry on the FM-tally (.07768667) is the atomic density of concrete
c given in atoms/barn/cm. The second entry is the material number (concrete).
c the final entry is the ENDF reaction number. 102 is the ENDF reaction number
c for the (n,gamma) activation reaction.
FMESH14:n      GEOM=XYZ     ORIGIN = 8.9 -1 -3.5
               IMESH=12.7   IINTS=19
   JMESH=1      JINTS=1
   KMESH=3.5    KINTS=35
FM14:n      .07768667        1      102
c ------------------------------------------------------------------------------
c Material Definition Section
c The syntax for the materials section is as follows:
c The first string of numbers is the isotope identifier, written in the form
c ZZZAAA. ZZZ being the atomic number of the isotope in question and AAA being
c its corresponding mass number. The second string (in this deck, the negative
c numbers below) specifies the atomic density of the isotope that precedes it
c in units of atoms/barn/cm
```

```
c           Concrete (KENO, regular mix)
c m1  1001  -0.0095    8016  -0.5054   14028  -0.32015 &
      13027 -0.0323    11023 -0.02755  20040  -0.0418  &
      26056 -0.0133    53127 -0.05     nlib=.70c
c -------1---------2---------3---------4---------5---------6---------7---------8
c The nps command specifies the number of particles simulated for this deck
nps 1e7
```

Appendix B: MCNP Code: Neutron Attenuation by Concrete

```
Analysing Attenuation properties of Concrete
c -------1---------2---------3---------4---------5---------6---------7---------8
c Analysis of neutron activation [(n,gamma) reaction] in a rectangular
c volume to test for the attenuation properties of the concrete used in this
c simulation. The neutron source was that of a directed plane source of thermal
c neutrons.
c -------1---------2---------3---------4---------5---------6---------7---------8
c Cell Cards
c The cell definition section consists mainly of the slab of concrete for this
c problem. The mass density of concrete is specified by the (-2.92) as the third
c string in the section below. The negative sign indicates a mass density is
c desired
c -------1---------2---------3---------4---------5---------6---------7---------8
c The second string should be changed according to the material present
c The accompanying density should be changed. Positive values denote an atomic
c density (atoms/barn/cm) while negative entries are for mass densities (g/cm^3)
10  1      -2.92      (-1)      imp:n=1    $(slab)
11  0                 (1 -100)  imp:n=1    $(external to slab)
20  0                 (100)     imp:n=0    $(end of world region)
c -------1---------2---------3---------4---------5---------6---------7---------8

c Surface Cards
c -------1---------2---------3---------4---------5---------6---------7---------8
c The geometry of interest is a 3.8-cm slab in a vacuum. The purpose is that
c attenuation will be isolated as the only effect of interest in the problem.
c -------1---------2---------3---------4---------5---------6---------7---------8
1  RPP  8.9 12.7  -1 1    -3.5 3.5
100 SO 30
c -------1---------2---------3---------4---------5---------6---------7---------8

c Data Cards
mode n
c -------1---------2---------3---------4---------5---------6---------7---------8
c Source Specification section
c The source is a directed thermal neutron plane source aimed at the front face
c of the concrete slab such that every emitted neutron is incident on the slab
```

```
c material.
SDEF  POS = 0 0 0 X=0 Y=d1 Z=d2 PAR=1 VEC=1 0 0 DIR=1 ERG=2.53e-8
SI1 -1 1
SP1 0    1
SI2 -1 1
SP2 0    1
c ------------------------------------------------------------------------------
c The tally that will be used is a rectangular F4 mesh tally modified by
c using an FM-multiplier card. The F4 tally measures the cell-averaged neutron
c flux in the cell of interest. The FM4 modifies this tally by multiplying the
c F4 tally by the microscopic absorption cross section
c
c The syntax of the rectangular mesh tally is as follows:
c FMESHn:<pl>   where n is the cell number and <pl> is the particle designator
c ORIGIN denotes the bottom left corner of the rectangle of that the tally will
c be defined in.
c IMESH is the placement along the x-axis of the coarse mesh points
c IINTS is the number of fine mesh points (bins) between the coarse mesh points.
c In the tally below, there are 19 bins being placed between 8.9-cm and 12.7-cm
c in the X direction.
c JMESH is the same as IMESH except in the y-axis.
c KMESH is the coarse mesh point in the z-axis
c
c The first entry on the FM-tally (.07768667) is the atomic density of concrete
c given in atoms/barn/cm. The second entry is the material number (concrete).
c the final entry is the ENDF reaction number. 102 is the ENDF reaction number
c for the (n,gamma) activation reaction.
c NOTE: WHEN A MATERIAL CHANGES, THE ATOMIC DENSITY TERM ALSO NEEDS TO BE
C ADJUSTED
FMESH14:n      GEOM=XYZ     ORIGIN = 8.9 -1 -1
               IMESH=12.7   IINTS=19
   JMESH=1      JINTS=1
   KMESH=1      KINTS=1
FM14:n      .07768667        1      102
c The mesh spacing is set so that the box is broken into .2cm thick increments
c in the x-direction
c The volume of each cell is equal to V = .2cm x 2cm x 2cm
c ------------------------------------------------------------------------------
```

```
c Material Definition Section
c The syntax for the materials section is as follows:
c The first string of numbers is the isotope identifier, written in the form
c ZZZAAA. ZZZ being the atomic number of the isotope in question and AAA being
c its corresponding mass number. The second string (in this deck, the negative
c numbers below) specifies the atomic density of the isotope that precedes it
c in units of atoms/barn/cm
c NOTE: UNCOMMENT THE MATERIAL OF INTEREST
c          Tagged Concrete (KENO, regular mix)
c        Atomic Density = .0782323746 atoms/barn/cm
c m1  1001  -0.0095    8016  -0.5054   14028  -0.32015 &
      13027 -0.0323    11023 -0.02755  20040  -0.0418  &
      26056 -0.0133    53127 -0.05     nlib=.70c
c         Untagged Concrete (KENO, regular mix)
c  Atomic Density = .07768667 atoms/barn/cm
c m2  1001  -.01       8016  -0.532    14028  -0.337   &
      13027 -0.034     11023 -0.029    20040  -0.044   &
  26056 -0.014                      nlib=.70c
c                     Iodine-127
c        Atomic Density = .00054571 atoms/barn/cm
c m3  53127 -1                        nlib=.70c
c -------1---------2---------3---------4---------5---------6---------7---------8
c The nps command specifies the number of particles simulated for this deck
nps 1e7
```

Appendix C: MCNP Code: Neutron Dispersion

```
Analysing Dispersion properties of Concrete
c -------1---------2---------3---------4---------5---------6---------7---------8
c Analysis of neutron activation [(n,gamma) reaction] in a rectangular
c volume to test for the dispersion properties of the concrete used in this
c simulation. The neutron source was a thermal point source at the origin.
c -------1---------2---------3---------4---------5---------6---------7---------8
c Cell Cards
c The cell definition section consists mainly of the slab of concrete for this
c problem. The mass density of concrete is specified by the (-2.92) as the third
c string in the section below. The negative sign indicates a mass density is
c desired
c -------1---------2---------3---------4---------5---------6---------7---------8
c The second string should be changed according to the material present
c The accompanying density should be changed. Positive values denote an atomic
c density (atoms/barn/cm) while negative entries are for mass densities (g/cm^3)
10  1      -2.92      (-1)      imp:n=1    $(slab)
11  0                 (1 -100)  imp:n=1    $(external to slab)
20  0                 (100)     imp:n=0    $(end of world region)
c -------1---------2---------3---------4---------5---------6---------7---------8

c Surface Cards
c -------1---------2---------3---------4---------5---------6---------7---------8
c The geometry of interest is a 7-cm long slab in a vacuum. The purpose is that
c dispersion will be isolated as the only effect of interest in the problem.
1  RPP  9 10  -3.5 3.5   -1 1
100 SO 30
c -------1---------2---------3---------4---------5---------6---------7---------8

c Data Cards
mode n
c -------1---------2---------3---------4---------5---------6---------7---------8
c Source Specification section
c The source is a thermal neutron point source at the origin
SDEF POS = 0 0 0 ERG=2.53e-8
c ------------------------------------------------------------------------------
c The tally that will be used is a rectangular F4 mesh tally modified by
```

```
c using an FM-multiplier card. The F4 tally measures the cell-averaged neutron
c flux in the cell of interest. The FM4 modifies this tally by multiplying the
c F4 tally by the microscopic absorption cross section
c
c The syntax of the rectangular mesh tally is as follows:
c FMESHn:<pl>   where n is the cell number and <pl> is the particle designator
c ORIGIN denotes the bottom left corner of the rectangle of that the tally will
c be defined in.
c IMESH is the placement along the x-axis of the coarse mesh points
c IINTS is the number of fine mesh points (bins) between the coarse mesh points.
c JMESH is the same as IMESH except in the y-axis and it is seen there are
c 34 mesh volumes generated to count the neutron activations.
c KMESH is the coarse mesh point in the z-axis
c
c The first entry on the FM-tally (.07768667) is the atomic density of concrete
c given in atoms/barn/cm. The second entry is the material number (concrete).
c the final entry is the ENDF reaction number. 102 is the ENDF reaction number
c for the (n,gamma) activation reaction.
c NOTE: WHEN A MATERIAL CHANGES, THE ATOMIC DENSITY TERM ALSO NEEDS TO BE
C ADJUSTED
FMESH14:n      GEOM=XYZ     ORIGIN = 9 -3.5 -1
               IMESH=10     IINTS=1
               JMESH=3.5    JINTS=34
               KMESH=1      KINTS=1
FM14:n      .0782323         1      102
c ------------------------------------------------------------------------------
c Material Definition Section
c The syntax for the materials section is as follows:
c The first string of numbers is the isotope identifier, written in the form
c ZZZAAA. ZZZ being the atomic number of the isotope in question and AAA being
c its corresponding mass number. The second string (in this deck, the negative
c numbers below) specifies the atomic density of the isotope that precedes it
c in units of atoms/barn/cm
c NOTE: UNCOMMENT THE MATERIAL OF INTEREST
c          Tagged Concrete (KENO, regular mix)
c        Atomic Density = .0782323746 atoms/barn/cm
c m1  1001  -0.0095    8016  -0.5054   14028  -0.32015 &
      13027 -0.0323    11023 -0.02755  20040  -0.0418  &
```

```
      26056 -0.0133    53127 -0.05     nlib=.70c
c         Untagged Concrete (KENO, regular mix)
c  Atomic Density = .07768667 atoms/barn/cm
c m2  1001  -.01       8016  -0.532    14028  -0.337   &
      13027 -0.034     11023 -0.029    20040  -0.044   &
  26056 -0.014                      nlib=.70c
c                     Iodine-127
c        Atomic Density = .00054571 atoms/barn/cm
c m3  53127 -1                        nlib=.70c
c -------1---------2---------3---------4---------5---------6---------7---------8
c The number of simulated particles was 1e7
nps 1e7
```

Appendix D: MCNP Code: Both Dispersion and Attenuation Present

```
Accounting for both Attenuation and Dispersion
c -------1---------2---------3---------4---------5---------6---------7---------8
c Analysis of neutron activation [(n,gamma) reaction] in a rectangular
c volume to test for the dispersion and attenuation properties of the concrete
c used in this simulation. The neutron source was a thermal point source at the
c origin.
c -------1---------2---------3---------4---------5---------6---------7---------8
c Cell Cards
c The cell definition section consists mainly of the slab of concrete for this
c problem. The mass density of concrete is specified by the (-2.92) as the third
c string in the section below. The negative sign indicates a mass density is
c desired
c -------1---------2---------3---------4---------5---------6---------7---------8
c The second string should be changed according to the material present
c The accompanying density should be changed. Positive values denote an atomic
c density (atoms/barn/cm) while negative entries are for mass densities (g/cm^3)
10  1      -2.92      (-1)      imp:n=1    $(slab)
11  0                 (1 -100)  imp:n=1    $(external to slab)
20  0                 (100)     imp:n=0    $(end of world region)
c -------1---------2---------3---------4---------5---------6---------7---------8

c Surface Cards
c -------1---------2---------3---------4---------5---------6---------7---------8
c The geometry of interest is a 7-cm wide, 3.8-cm thick
c slab in a vacuum. The purpose is that both attenuation and dispersion will be
c accounted for.
1  RPP  8.9 12.7  -1 1   -3.5 3.5
100 SO 30
c -------1---------2---------3---------4---------5---------6---------7---------8

c Data Cards
mode n
c -------1---------2---------3---------4---------5---------6---------7---------8
c Source Specification section
c The source is a thermal neutron point source at the origin
SDEF POS = 0 0 0 ERG=2.53e-8
```

```
c ------------------------------------------------------------------------------
c The tally that will be used is a rectangular F4 mesh tally modified by
c using an FM-multiplier card. The F4 tally measures the cell-averaged neutron
c flux in the cell of interest. The FM4 modifies this tally by multiplying the
c F4 tally by the microscopic absorption cross section
c
c The syntax of the rectangular mesh tally is as follows:
c FMESHn:<pl>   where n is the cell number and <pl> is the particle designator
c ORIGIN denotes the bottom left corner of the rectangle of that the tally will
c be defined in.
c IMESH is the placement along the x-axis of the coarse mesh points
c IINTS is the number of fine mesh points (bins) between the coarse mesh points.
c JMESH is the same as IMESH except in the y-axis and it is seen there are
c 34 mesh volumes generated to count the neutron activations.
c KMESH is the coarse mesh point in the z-axis
c
c The first entry on the FM-tally (.07768667) is the atomic density of concrete
c given in atoms/barn/cm. The second entry is the material number (concrete).
c the final entry is the ENDF reaction number. 102 is the ENDF reaction number
c for the (n,gamma) activation reaction.
c NOTE: WHEN A MATERIAL CHANGES, THE ATOMIC DENSITY TERM ALSO NEEDS TO BE
C ADJUSTED
FMESH14:n      GEOM=XYZ     ORIGIN = 8.9 -1 -3.5
               IMESH=12.7    IINTS=19
               JMESH=1       JINTS=1
               KMESH=3.5     KINTS=34
FM14:n      .0782323         1      102
c ------------------------------------------------------------------------------
c Material Definition Section
c The syntax for the materials section is as follows:
c The first string of numbers is the isotope identifier, written in the form
c ZZZAAA. ZZZ being the atomic number of the isotope in question and AAA being
c its corresponding mass number. The second string (in this deck, the negative
c numbers below) specifies the atomic density of the isotope that precedes it
c in units of atoms/barn/cm
c NOTE: UNCOMMENT THE MATERIAL OF INTEREST
c          Tagged Concrete (KENO, regular mix)
c        Atomic Density = .0782323746 atoms/barn/cm
```

```
c m1  1001  -0.0095    8016  -0.5054   14028  -0.32015 &
      13027 -0.0323    11023 -0.02755  20040  -0.0418  &
      26056 -0.0133    53127 -0.05     nlib=.70c
c         Untagged Concrete (KENO, regular mix)
c  Atomic Density = .07768667 atoms/barn/cm
c m2  1001  -.01       8016  -0.532    14028  -0.337   &
      13027 -0.034     11023 -0.029    20040  -0.044   &
  26056 -0.014                      nlib=.70c
c                     Iodine-127
c        Atomic Density = .00054571 atoms/barn/cm
c m3  53127 -1                        nlib=.70c
c -------1---------2---------3---------4---------5---------6---------7---------8
c The number of simulated particles was 1e7
nps 1e7
```

Appendix E: MATLAB code used to plot MCNP results

```
% Defining the excel sheets where MCNP data was stored
file1 = 'rectangle_mesh_untagged.xlsx';
file2 = 'rectangle_mesh_tagged.xlsx';
%%%%%%%%%%%%%%%%%%%%%%%%%%%%%%%%%%%%%%%%%%%%%%%%%%%
% Extracting relevant data from excel files
x_1 = xlsread(file1,1,'A2:A36');
h_1 = xlsread(file1,1,'B1:T1');
A_1 = xlsread(file1,1,'B2:T36');

x_2 = xlsread(file2,1,'A2:A36');
h_2 = xlsread(file2,1,'B1:T1');
A_2 = xlsread(file2,1,'B2:T36');
%%%%%%%%%%%%%%%%%%%%%%%%%%%%%%%%%%%%%%%%%%%%%%%%%%%



% Plotting features from variables above
figure; hold on
surf(h_1,x_1,A_untag)
surf(h_2,x_2,A_tag)
colorbar('location','EastOutside')
c = colorbar;
view([-135 20])
axis tight
load zLimits
zlim(zLimits);
rotate3d on
xlabel('height from central axis (cm)');
ylabel('horizontal distance along slab(cm)');
zlabel('volumetric activation rate (atoms/SP/cm^3)');%
title('MCNP Results for Tagged & Untagged Concrete');
%%%%%%%%%%%%%%%%%%%%%%%%%%%%%%%%%%%%%%%%%%%%%%%%%%%
% The result matrices for the tagged and untagged
% Concrete are subtracted from each other to give
% the total number of activations due to the
% Iodine tag for each of the mesh tally cells.
A_3 = A_2 - A_1;
```

```
A_diff = A_3 .*(3.7 * 10^(10));
surf(h_1,x_1,A_diff)
colorbar('location','EastOutside')
c = colorbar;
axis tight
rotate3d on
xlabel('height from central axis (cm)');
ylabel('horizontal distance along slab (cm)');
zlabel('added activations (^{128}I atoms/Ci/cm^3)');
title('Difference in activations for Tagged & Untagged Concrete');
```

Appendix F: MATLAB code used to theoretically predict activations

```
%Constant definition section
sigma_1 = .0033834;
%macroscopic thermal absorption cross section for I-127 (1/cm)
sigma_2 = .0132971326;
%macroscopic thermal absorption cross section for Tagged Concrete
sigma_3 = .00991373;
%macroscopic thermal absorption cross section for Untagged Concrete
r_in = 8.9;             %inner radius of the annulus (cm)
%variables of interest
x1 = 9:.2:12.6;         %distance away from source in the x-direction (cm)
h1 = -3.4:.2:3.4;       %vertical distance from source (cm)
d = .1:.2:3.6;          %depth into slab (cm)
x = length(x1);
h = length(h1);
phi=zeros(x,h);
R = zeros(x,h);
% Calculating the flux term for each of the cell volumes
for i=1:x
for j=1:h
R(i,j) = sqrt(x1(i)^2 + h1(j)^2);
d(i,j) = R(i,j) - (r_in .* R(i,j))./x1(i);
phi(i,j) = 1/((4*pi).*R(i,j).^2) .* exp(-sigma_2 .* d(i,j));
end
end
%Generating a matrix whose entries are the number of neutron activations in
%a cell. For different materials present, use the corresponding macroscopic
%absorption cross section (sigma_1, sigma_2, or sigma_3)
A_1 = phi.*sigma_2;

% Plotting results matrix
figure; hold on
surf(h1,x1,A_1)
surf(h1,x1,A_2)
colorbar('location','EastOutside')
c = colorbar;
rotate3d on
```

```
% xlim([-3.4 3.4]);
% ylim([9 12.6]);
axis tight;
view([-45 20])
load zLimits
zlim(zLimits);
xlabel('height from central axis (cm)');
ylabel('horizontal distance along slab(cm)');
zlabel('volumetric activation rate (atoms/SP/cm^3)');
title('Predicted Results for Untagged & Tagged concrete');
```

References

[1] Baskaran, R. et al. "Analysis of neutron streaming through the trenches at linac based neutron generator facility, IGCAR." *Radiation Protection and Environment* 34:4 (2011): 262-266. Accessed April 30, 2014. doi: 10.4103/0972-0464.106194.

[2] Burgett, E. et al. "Study of a gold-foil based multisphere neutron spectrometer." *Radiation Protection Dosimetry* 128:3 (2008): 289-293. Accessed April 30, 2014. doi:10.1093/rpd/ncm375.

[3] Environmental Protection Agency. "Electrical Methods." Last modified December 12, 2011.

`epa.gov/esd/cmb/GeophysicsWebsite/pages/reference/methods/Borehole_Geophysical_Methods/.`

[4] Environmental Protection Agency. "Nuclear Logging." Last modified December 12, 2011.

`http://www.epa.gov/esd/cmb/GeophysicsWebsite/pages/reference/methods/.`

[5] Korean Atomic Energy Research Institute. "Table of Nuclides." Last modified 2000.

`http://atom.kaeri.re.kr/ton/index.html.`

[6] Krauss, Clifford and Campbell Robertson. "Gulf Spill is the Largest of Its Kind, Scientists Say." *The New York Times,* August 2, 2010. Accessed April 15, 2014.

`http://www.nytimes.com/2010/08/03/us/03spill.html?_r=1&fta=y.`

[7] Los Alamos National Laboratory. *MCNP6 User's Manual: Version 1.0.* By Thomas E. Booth et al. LA-CP-13-00634. Los Alamos , New Mexico: Los Alamos National Laboratory, 2013.

[8] Mathworks. "MATLAB." Last modified 2014.

`http://www.mathworks.com/products/matlab/.`

[9] Miraglia, Peter. *Scoping Analysis of Neutron Activation In-Situ Technique for Inspection of Oil Well Casing Cement for Volume Defects.* Cambridge: March 10, 2014.

[10] National Commission on the BP Deepwater Horizon Oil Spill and Offshore Drilling. *Deepwater: The gulf Oil Disaster and the Future of Offshore Drilling.* By Bob Graham, et al. Washington, D.C.: United States Government Printing Office, January 2010.

[11] Neutron Activation Analysis Online. "Introduction".

`http://www.naa-online.net/theory/introduction/.`

[12] Oilfield Glossary. "Resistivity Log." Last modified 2014.

http://www.glossary.oilfield.slb.com/en/Terms/r/resistivity_log.aspx.

[13] Rambow, Frederick. 1991. Radioactive Tracer Cement Thickness Measurement. U.S. Patent 5,001,352. Filed June 20, 1989. Issued March 19, 1991.

[14] Robertson Geologging. "History." Last modified 2014.

http://welllogging.co.uk/history-well-logging/.

[15] Schlumberger. "Resistivity Log." Last modified 2014.

http://www.glossary.oilfield.slb.com/en/Terms/r/resistivity_log.aspx

[16] Schlumberger. "Trends in NMR Logging." Last modified 2014.

http://www.slb.com/resources/publications/industry_articles/oilfield_review/2000/.

[17] Turner, James E. *Atoms, Radiation, and Radiation Protection.* KGaa, Winheim: Wiley-VCH Verlag GmbH & Co., 2012.

[18] Welltec. "Caliper Logging." Last modified 2014.

http://www.welltec.com/Caliper-Logging.aspx?ID=70.

[19] Welltec. "Cement Bond Logging." Last modified 2014.

http://www.welltec.com/Cement-Bond-Logging.aspx?ID=75.